HARRIS®

TECHNOLOGY TO CONNECT, INFORM AND PROTECT™

Continuous Phase Modulation for GPS Codes: Reducing Out-of-band Emissions and Improving RF/DC Efficiency

Philip Kossin, Jan Zygmaniak and Theodore Guasconi

Harris Corporation
Space and Intelligence Systems

TABLE OF CONTENTS

LIST OF FIGURES

Continuous Phase Modulation for GPS Codes: Reducing Out-of-band Emissions and Improving RF/DC Efficiency

SUMMARY

The standard definitions of GPS signals [1][2] [3] are ideal binary phase shift keying (BPSK) or quadrature phase-shift keying (QPSK) phase modulated carriers. According to these ideal definitions, the GPS waveforms should only modulate the phase of the RF carrier, yielding a constant envelope signal suitable for high efficiency, saturated amplification. As a result, saturated power amplifiers (HPAs) are favored in GPS navigational payloads to minimize power consumption. The problem is that ideal waveforms would need to occupy infinite bandwidth to keep their constant envelope.

In a hardware implementation, the finite bandwidth of the channel gives rise to envelope variations that reduce the efficiency and power output of the saturated amplifier. Additionally, these ideal high-bandwidth signals have significant frequency content well outside the system operational bandwidth. The result is wasted RF power and the need to use bandpass filters at the HPA output to comply with out-of-band spectral requirements. The design of these filters is complicated by simultaneous requirements for high rejection of frequencies close to the operating band, ability to tolerate high power levels, and low insertion loss. Filtering the signal before the HPA may not sufficiently reduce the out-of-band spectral energy of the amplified signal due spectral regrowth from the nonlinear HPA.

These same issues are common to many RF communication systems. To address the problem, continuous phase modulation (CPM) waveforms were developed. CPM operates in the phase domain to smooth the phase transitions of the signal to reduce the bandwidth but keep the envelope constant. CPM signals achieve reduced bandwidth at the output of a saturated HPA, while providing acceptable communication efficiency for data links.

While it is logical to consider using CPM for GPS/GNSS applications, these navigational applications present unique challenges. The large number of existing receivers require that changes to the currently transmitted waveforms be compliant with system requirements and have little or no degradation for existing user equipment. Navigation systems like GPS rely on the correlation of the signal at the receiver to accurately estimate time and range from the satellite. Any modifications to the waveform must preserve the quality of the correlation to maintain accurate time and ranging estimates.

This article discusses a method of applying known CPM techniques to the GPS/GNSS navigational system in such a way as to be compatible with legacy equipment, while reaping the benefits of improved spectral and DC efficiency. Attention is given to the unique requirements of a GPS or other navigational system that differentiate it from a communication system. A method is presented that both maintains the spectral efficiency of CPM and remains in compliance with correlation loss and preserving the quality of the correlation function in legacy receivers. This work primarily focuses on the design of a CPM version of the BOC(10,5) signal, but also includes results for the C/A and P code modulation. Hardware testing of the CPM version of the BOC(10,5) signal amplified with flight-like HPAs demonstrates that the anticipated spectral efficiency is achieved while providing improved DC efficiency over the conventional BPSK waveforms.

The GPS Transmission Architecture

A simplified architecture of the GPS RF transmission system is presented in Figure 1 for the reader to understand the desired characteristics of the modulation.

GPS transmission architectures typically consist of the following functions, shown in the block diagram in in Figure 1 below:

- **GPS Code Generator**: Generates binary PRN sequence with NAV message
- **Waveform Generator:** Converts binary output from the Code Generator into baseband digital modulation
- **L-band Upconverter**: Shifts baseband signal up to L-band carrier frequency to produce modulated L-band signal
- **HPA:** Amplifies modulated L-band signal from upconverter to desired RF power level of GPS signal
- **Bandpass Filter:** Rejects out of band energy of HPA output for spectral compliance
- **Antenna**

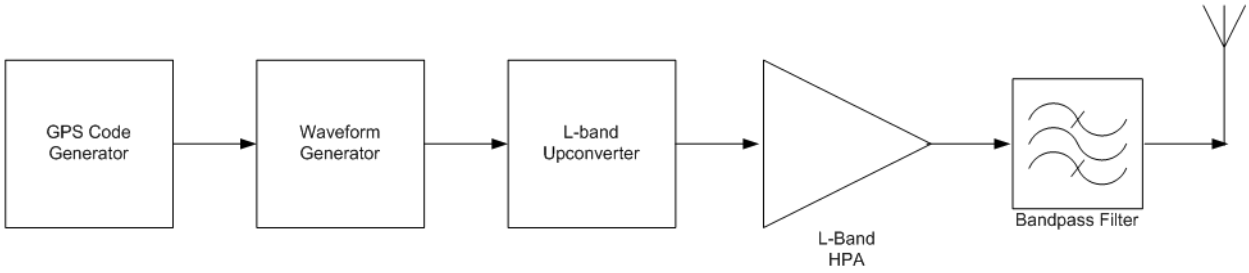

Figure 1: Simplified GPS RF transmission system architecture

Reduced Efficiency and Maximum HPA Power Due to Envelope Variations

In a conventional GPS implementation, the waveform generator modulates the binary output of the code generator using the phase modulation specified in the relevant ICD/system specification [1]. For the BOC(10,5) code this is BPSK. The ideal modulated BOC(10,5) signal should be a constant-envelope waveform with rectangular phase symbols. Figure 4 contains the spectrum of the ideal ICD version of the BOC(10,5) signal. The spectrum of the ideal signal extends over all frequencies, so an infinitely wide channel would be needed to faithfully reproduce the ideal signal in hardware. Since all real hardware has a finite bandwidth, the higher frequency components of the baseband modulated signal will be lost or attenuated. This results in a signal that no longer has a constant envelope. The higher the percentage of power that resides at frequencies outside the channel bandwidth, the greater the envelope variation. Because the BPSK signal has so much high frequency content, the envelope variation is significant.

To illustrate this point, we simulated an ideal BPSK BOC(10,5) signal that has been modulated at the L1 frequency and then passed through a bandpass filter to simulate a 200MHz channel bandwidth. Figure 2 contains the time domain waveform of the filter output. The envelope of the RF signal can be seen to collapse at the symbol transitions, meaning that the instantaneous power of the signal drops to zero at these times.

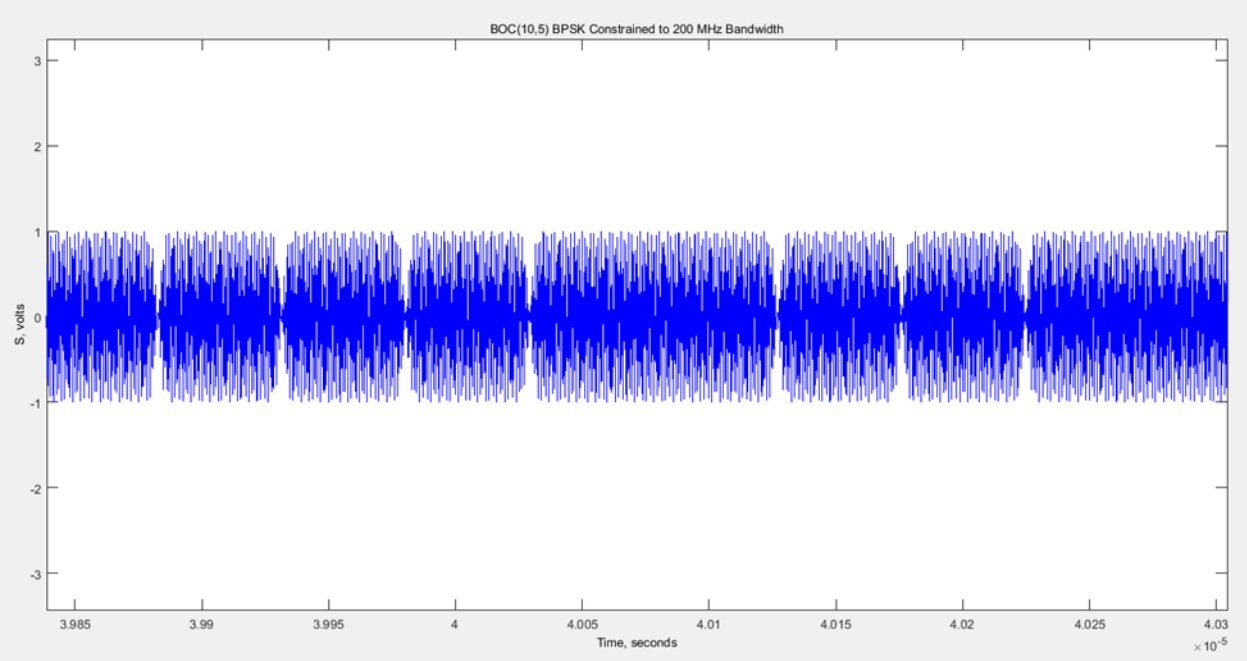

Figure 2: Simulated BPSK BOC(10,5) signal constrained to 200 MHz bandwidth. Note envelope variations appear as notches during phase transitions

For maximum efficiency, RF amplifiers for GPS transmission systems typically operate several dB into gain compression. But with this band-limited BPS signal, even if the RF amplifier is set up to run at an efficient, gain-compressed operating point during most of the waveform, it will be backed off from that operating point as the envelope collapses at the transitions. This corresponds to a decreased average efficiency of the HPA. Since physical hardware has a finite bandwidth, an HPA operating in compression shows a lower efficiency for a BPSK signal than for a carrier wave (CW) carrier. The extent of this drop depends the code symbol rate and the hardware bandwidth. Figure 3 shows hardware test data for an L-band GaN HPA amplifying a CW and BPSK BOC(10,5) signal. The degradation in efficiency can be seen by comparing the CW and BPSK curves in Figure 3. Note that BPSK has a lower efficiency than CW at the higher power levels where the HPA is in compression.

Another performance degradation caused by the envelope variations is a drop in the max power output capability of the HPA. Note from the power output (Pout) curve in Figure 3 that the maximum output power of the HPA is lower for BPSK than for CW. This is because the reduced envelope during symbol transitions decreases the average power of the signal. Increasing the drive will not increase the output power past this point because the device is already in saturation.

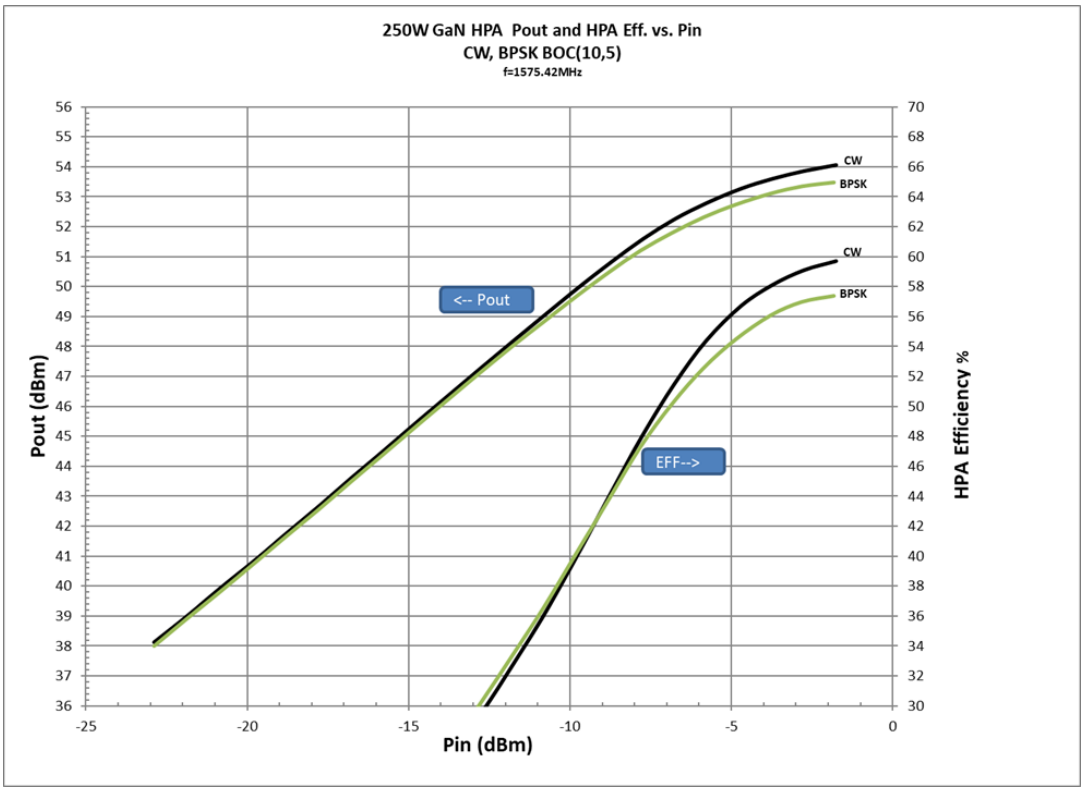

Figure 3: 250W GaN HPA output power and efficiency for CW and BPSK BOC(10,5)

Filter Losses Due to Out-of-Band Emissions

The diagram in Figure 1 includes a bandpass filter following the HPA. The purpose of this filter is to reduce the out-of-band emissions so that the transmitted signal is compliant with spectral requirements. The losses introduced by this filter consist of truncation loss and insertion loss:

$$(L\_filter)_{dB} = (L\_truncation)_{dB} + (L\_insertion)_{dB}$$

Truncation Loss

Figure 4 shows the theoretical HPA output spectrum for a BOC(10,5) BPSK signal compared to the GPS operational bandwidth of 30.69MHz. Filtering must be applied to suppress the energy outside of the operational bandwidth to comply with out-of-band emissions requirements. The fraction of out-of-band power that is removed by the filtering action is called truncation loss. This power is outside of the GPS operational bandwidth and would not have been useful to a GPS receiver. However, a portion of DC power was consumed in the HPA to generate this unusable power. Therefore, truncation loss represents a reduction in system efficiency. The truncation loss for a BPSK BOC(10,5) signal is 1.16dB when using an ideal "brick wall" filter with a bandwidth of 30.69MHz. We will show that CPM reduces this loss later in this paper.

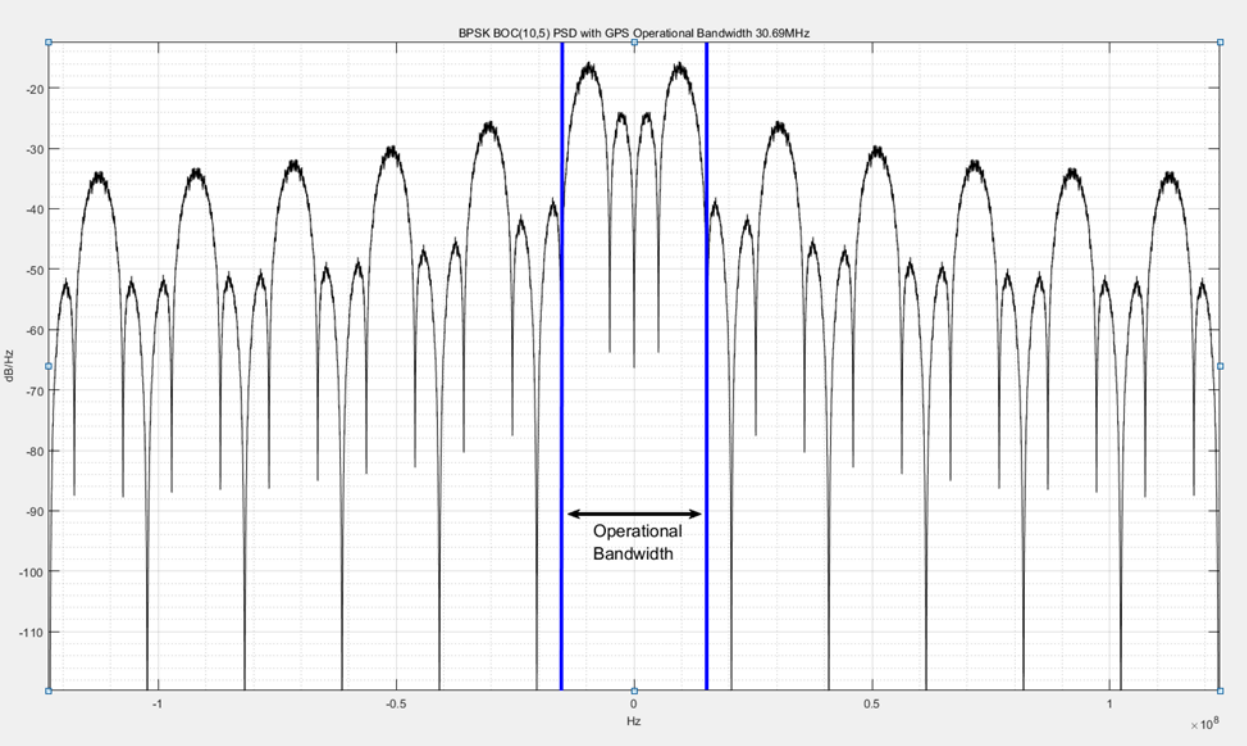

Figure 4: Simulated power spectrum of BOC(10,5) with standard BPSK modulation showing GPS operational bandwidth

Insertion Loss

The high-power bandpass filter must have steep rejection on each side of the passband to suppress the significant out-of-band emissions of the BPSK signal to meet spectral requirements. The greater the rejection need from the filter, the greater the number of poles. The additional poles required for filtering the wide bandwidth BPSK modulation typically correspond to higher insertion loss. This additional loss further reduces system efficiency.

Spectral Regrowth

One solution that comes to mind is to move the filter to the input of the HPA. However, the nonlinearity of the high-efficiency HPA causes a re-growth of most of the original BPSK spectrum at its output. Therefore, an output filter with its inherent losses would still be needed after the HPA. To make matters worse, filtering at the input to the HPA results in additional envelope variation and the inherent degradation to RF/DC efficiency of the HPA discussed previously. Operating the HPA in a linear region would solve this problem, but at the expense of reduced efficiency.

Design Objectives for an Improved GPS Modulation

Our technical challenge is to design a modified version of the GPS waveform that overcomes the issues described above.

In summary, we seek to produce a modulated GPS signal with the following qualities:

- Constant envelope
- Reduced bandwidth
- Minimal spectral growth after amplification by saturated HPA

- Compatibility with legacy user equipment
- Compliant with ICD requirements

Application of CPM to GPS Signals

The constellation diagram for BPSK is shown in Figure 5. The modulated signal transitions between the two symbol possibilities based on the pseudo-noise (PN) sequence defined for the GPS code. For ideal BPSK, the phase transitions instantaneously from 0 to π when the data changes from a '1' to a '0', and vice versa.

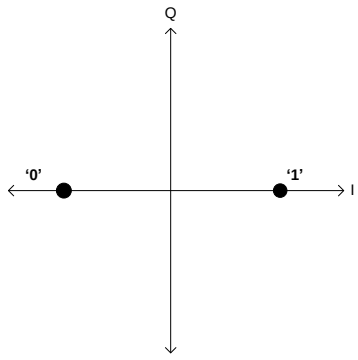

Figure 5: BPSK signal in I-Q space

The black trace shown in Figure 6 is the time domain plot of the phase trajectory of BPSK modulation. The phase transition consists of a step function that increases instantly from 0 to 180 degrees. The wide spectrum of the BPSK-modulated GPS signals shown in Figure 4 results from the high-frequency content of these instantaneous phase transitions.

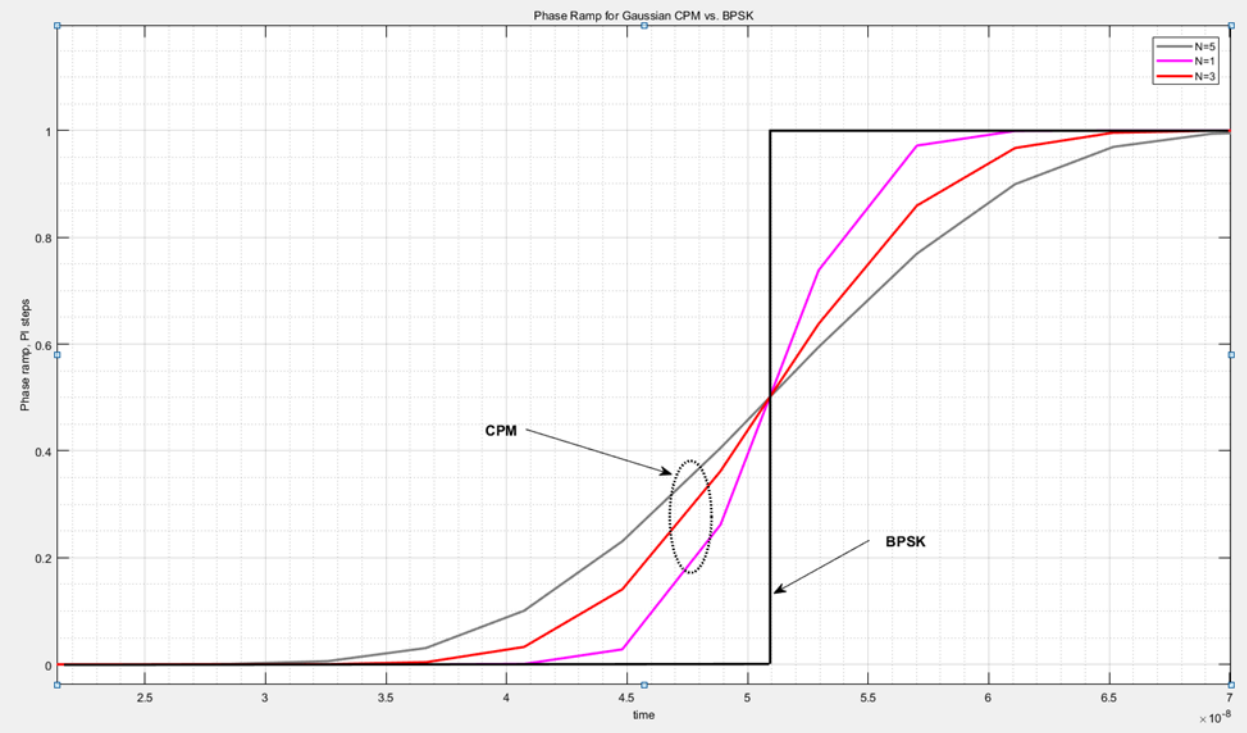

Figure 6: Simulated phase transitions for (Gaussian) CPM vs. BPSK

CPM is a class of digital modulations that achieves bandwidth efficiency while maintaining a constant envelope. The generalized expression for a CPM signal is defined in [6] as:

$$S(t) = R_e\left(Ae^{j\omega t+\emptyset(t)}\right) \quad (1)$$

Where

A is the constant amplitude of the modulated carrier

$$\emptyset(t;I) = 2\pi \sum_{k=-\infty}^{n} I_k \, h_k q(t - kT)$$

I_k – *sequence of M-ary symbols: ±1, ±3, …, ±(M-1)*

h_k – *sequence of modulation indices*

$q(t)$ – *normalized pulse shape*

For our application, the BOC(10,5) code is binary PSK, so M=2. The absolute starting phase of the modulation is arbitrary since the channel between the transmitter and receiver will introduce an unknown phase error, and the receiver uses the magnitude of the complex correlation of the incoming and reference signal for the time/range estimate. We can therefore define the waveform as a differential modulation as follows:

$$\emptyset(\boldsymbol{t};\boldsymbol{I}) = \boldsymbol{2\pi} \sum_{\boldsymbol{k=-\infty}}^{\boldsymbol{n}} \boldsymbol{I_k \, h_k q(t - kT)}$$

$$= \emptyset_i + \boldsymbol{\pi} \sum_{\boldsymbol{k=-\infty}}^{\boldsymbol{n}} \Delta_k \, \boldsymbol{q(t - kT)}$$

Where

$\emptyset_i$ is the arbitrary initial absolute phase

and

$$\Delta_k = \begin{cases} \mathbf{0}, \boldsymbol{code\ phase\ dwell} \\ \pm\mathbf{1}, \boldsymbol{code\ phase\ shift} \end{cases}$$

If the NAV PN code is a series of BPSK symbols such that +1 represents a phase of 0 degrees and -1 represents a phase of 180 degrees, then:

PN=d_k where $d_k = \pm 1$

So

$$\Delta_k = \pm \left| \frac{d_k - d_{k-1}}{2} \right|$$

So that Δ_k can be derived from the NAV PN code.

The pulse shape q(t) is selected to provide a smoothed, continuous phase trajectory for the transmitted signal. This avoids the sudden phase transitions of BPSK and results in a more bandwidth efficient signal. In the current work we generated q(t) by integrating a Gaussian frequency pulse. This is the same method used in generating GMSK modulation. We will refer to this form of CPM as Gaussian CPM or GCPM.

The colored traces in Figure 6 are the phase trajectories of Gaussian CPM modulation using varying degrees of phase trajectory smoothing. Figure 7 shows a block diagram of the Gaussian CPM modulation process used to generate the CPM waveforms investigated here. The number of samples N in the duration of the rectangular pulse at the input to the Gaussian filter, and BT, the bandwidth of the Gaussian filter, are used to control the degree of smoothing of the phase transitions. For the results presented, the total number of samples per symbol L=12. For example, a waveform with N=5 means that the filter input pulse width was 5 samples out of the total possible 12 samples in each symbol. If a different number of samples per symbol were used, the ratio N/L and BT would determine the trajectory smoothing.

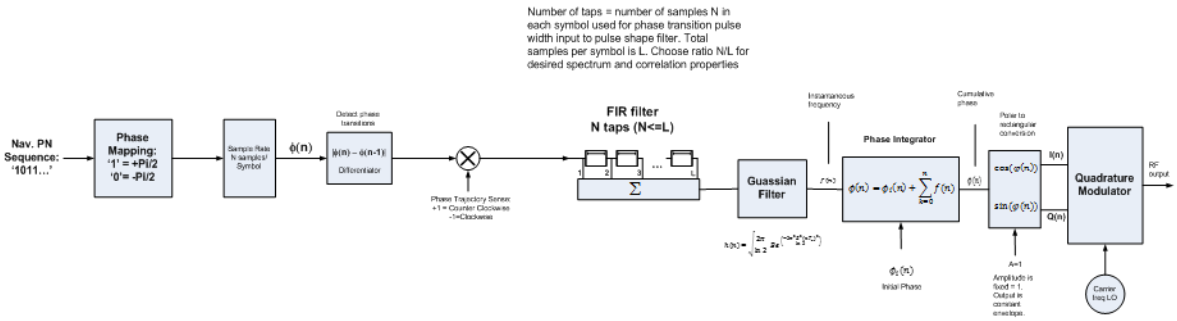

Figure 7: Gaussian CPM modulator for BPSK GPS codes

The next step is to look at the signal in I-Q space during transitions. As shown in Figure 5, the modulation is a constant-envelope binary CPM, meaning that the phase will transition between the two symbols shown along a circle, with the radius equal to the RF envelope level. Figure 8 shows an example vector diagram. When transitioning from symbol '1' to '0' with a constant envelope modulation, there are two possible phase paths:

[1] Transition in the counterclockwise direction around the upper half of the unit circle, as shown in Figure 8

[2] Transition in the clockwise direction around the lower half of the unit circle, as shown in Figure 9

And similarly, when transitioning from a symbol '1' to a symbol '0'.

As we continue to transition between multiple symbols over the entire PN code sequence, the following phase transition possibilities emerge:

Case 1: Transition in phase in the counterclockwise direction (positive phase step) (+, +, +…) – see Figure 10

Case 2: Transition in phase in the clockwise direction (negative phase step) (–, –, –…) – see Figure 11

Case 3a, 3b: Alternate between clockwise and counterclockwise (Transition back from '1' to '0' along the same path used to transition from '0' to '1') (–, +, –, +…) – see figures 12 and 13

Case 4: A combination of clockwise and counterclockwise transitions following a predetermined pattern. For example, the pattern may be based on a PN sequence.

First, we will analyze cases 1, 2, and 3.

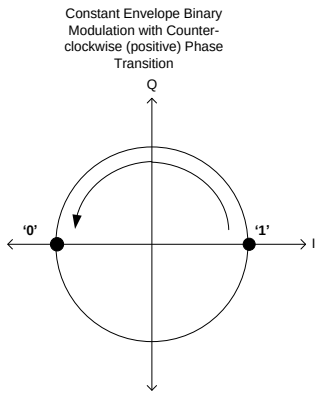

Figure 8: Constant-envelope binary CPM, positive (counterclockwise) phase transition

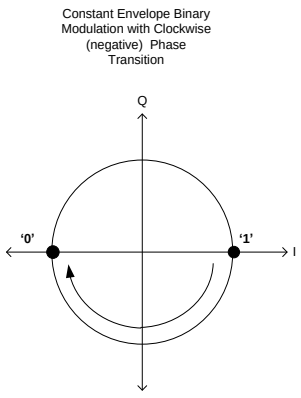

Figure 9: Constant-envelope binary CPM, negative (clockwise) phase trajectory

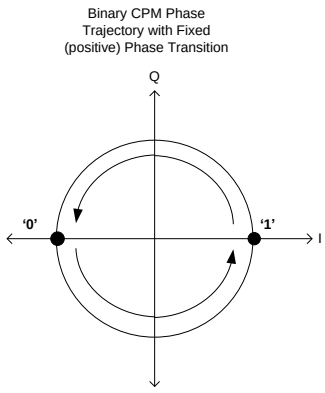

Figure 10: Case 1: Constant-envelope binary CPM, positive phase transitions for all symbols

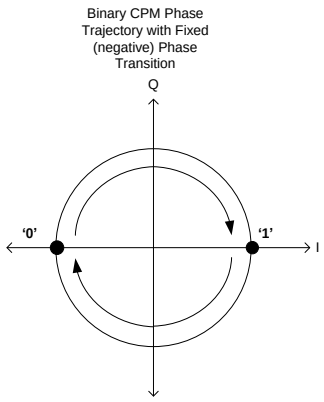

Figure 11: Case 2: Constant-envelope binary CPM, negative phase transitions for all symbols

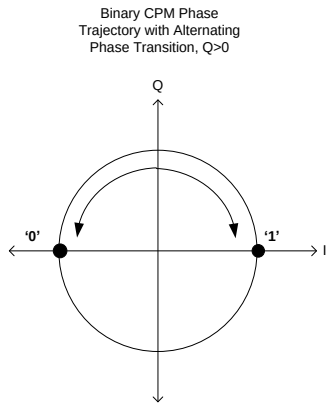

Figure 12: Case 3a: Constant-envelope binary CPM, alternating polarity phase transitions, upper half plane

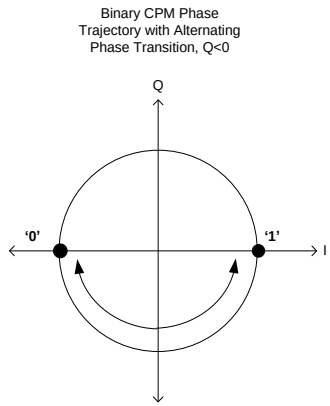

Figure 13: Case 3b: Constant-envelope binary CPM, alternating polarity phase transitions, lower half plane

Cases 1 and 2: Continuous Phase Accumulation (Positive or Negative)

In Cases 1 and 2, the direction of the phase trajectory is either always positive (counterclockwise rotation) or always negative (clockwise rotation), as shown in Figures 10 and 11.

Figure 14 shows the time domain phase ramp of Case 1, where the phase transitions are always positive. Even though the phase ramp is data dependent, there is not always a phase transition between symbols. Over multiple symbols, however, there is an average positive phase slope over the course of the sequence. This positive phase slope corresponds to a positive frequency shift of the portion of the signal energy, which resides in the symbol transition.

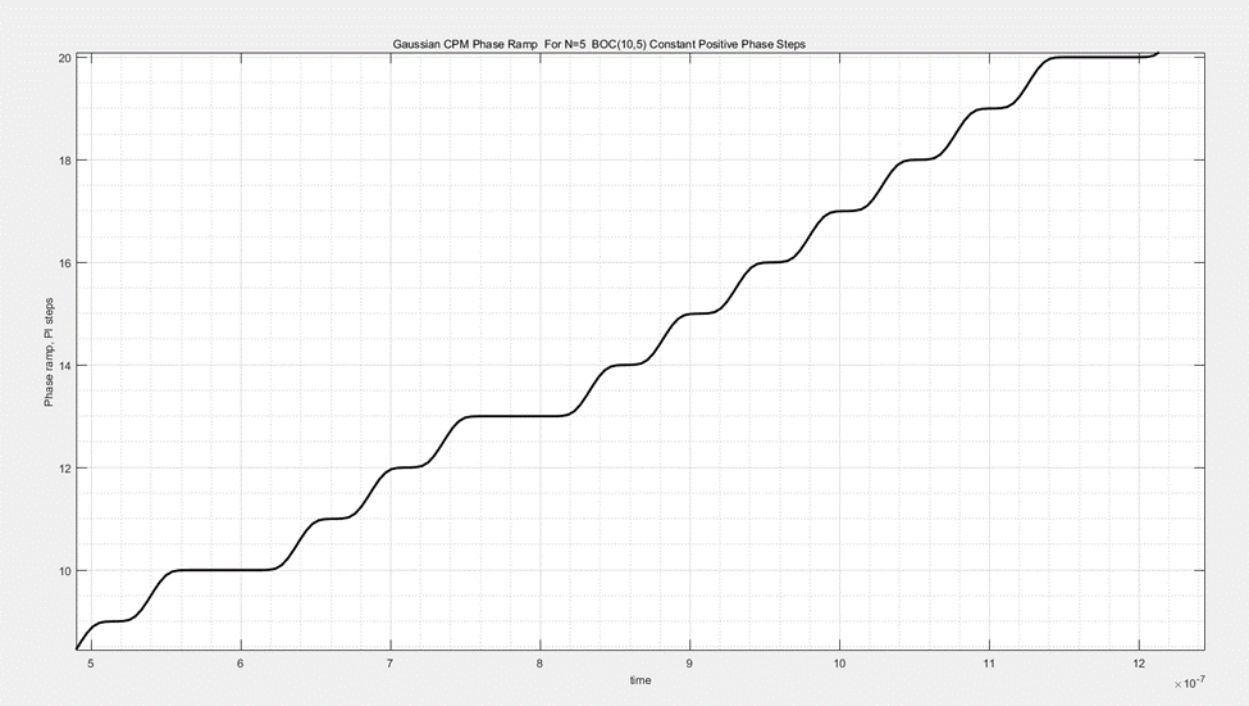

Figure 14: Phase trajectory for Gaussian CPM modulation with all positive (counterclockwise) phase steps (Simulation)

Figure 15 depicts the power spectrum of this same waveform. Compared to the BPSK BOC(10,5) spectrum, the power in frequencies higher than the carrier have been increased, while the power below the carrier frequency has been decreased. This is consistent with a positive average phase ramp, as explained above. We see the opposite effect for a fixed negative phase step where the power has shifted to the lower frequencies in Figure 16.

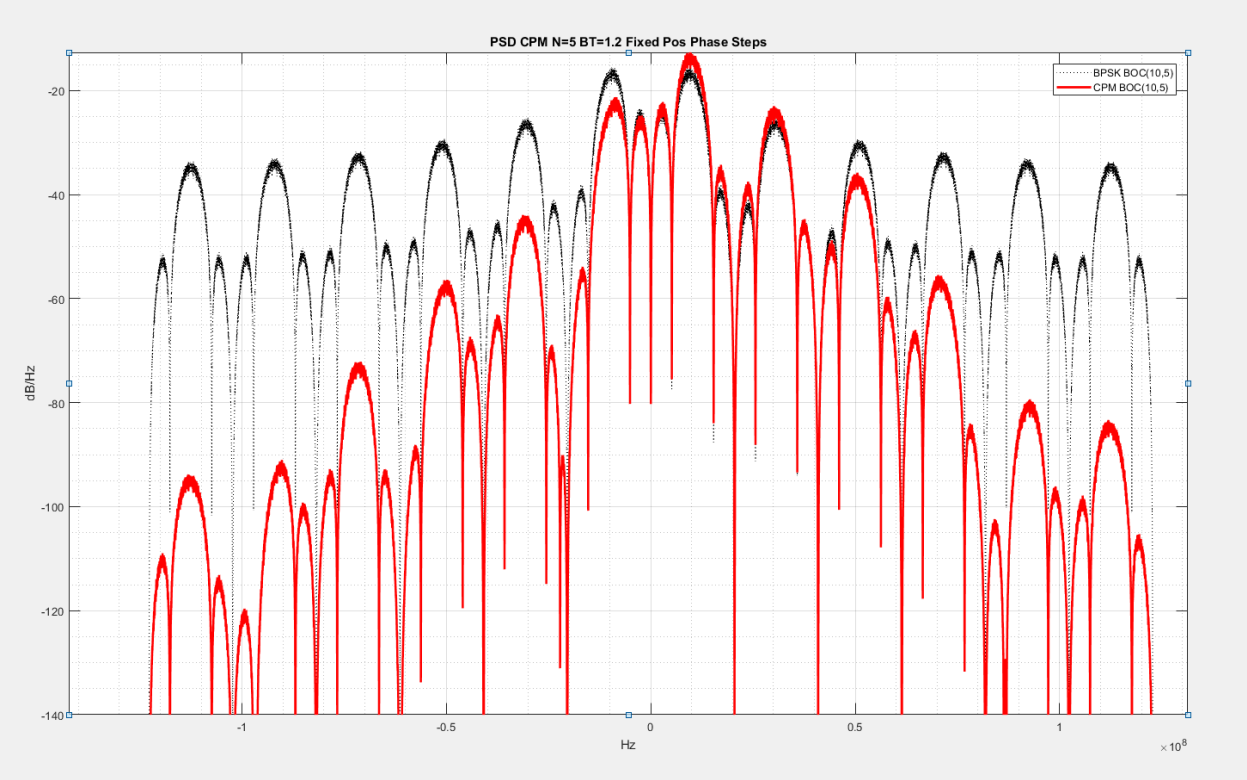

Figure 15: PSD for N=5, BT=1.2, Gaussian CPM with fixed positive polarity phase steps (simulation)

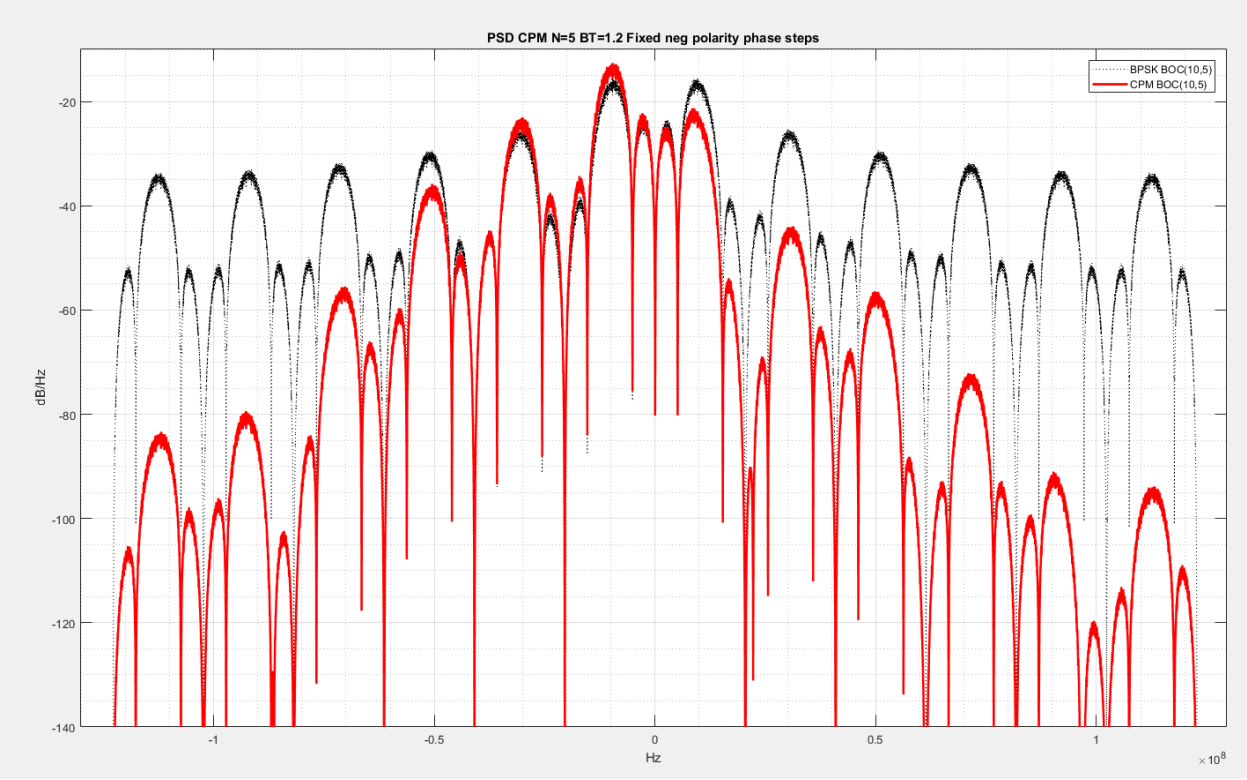

Figure 16: PSD for N=5, BT=1.2, Gaussian CPM fixed negative polarity phase steps (simulation)

GNSS modulation studies typically use plots of the autocorrelation function (ACF) as a figure of merit. Since our goal is to develop a waveform compatible with existing receivers, we use the cross-correlation between the receiver local reference code (BPSK) stored in the receiver and the CPM waveform from the transmitter. Figure 17 includes this type of cross-correlation. Note from the figure that the deep nulls at half-symbol offsets of the M-code ACF have been replaced by much shallower nulls in the CPM version. This is not acceptable since it will degrade the accuracy of the range estimate.

The explanation for this filling-in of the correlation nulls is that some of the energy from each symbol is spilling over into the adjacent symbol during the phase transition. This can be understood graphically by referring to Figure 10. There, when the signal transitions from a '1' to '0', the Q channel will have a positive pulse during the phase transition between symbols, which is the same as the previous symbol, data '1', and when transitioning from '0' to '1' the Q channel will have a negative pulse during the transition, which is the same as the previous symbol, data '0'. This means that previous symbol energy is still present in the Q channel during the phase transition, which gives rise to the degraded null depths at the half-symbol offsets.

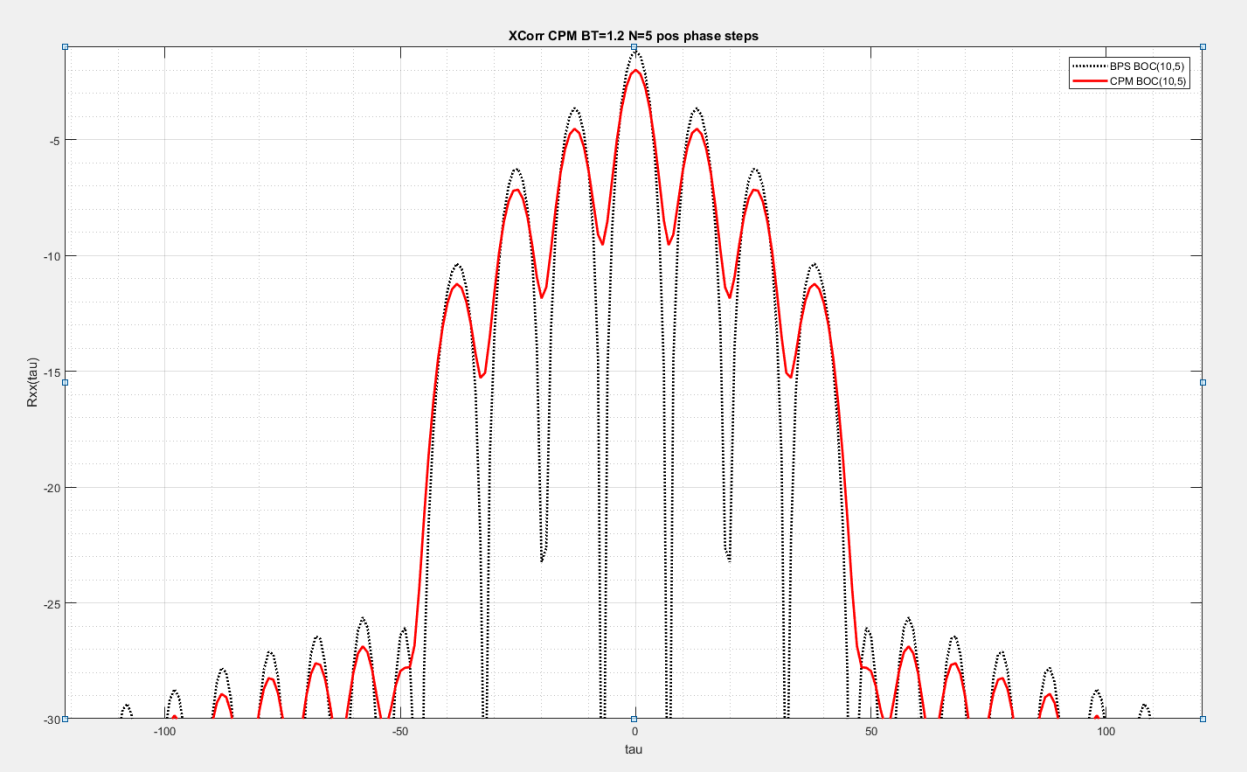

Figure 17: Correlation between reference and Gaussian CPM with fixed (positive or negative) polarity phase steps (simulation)

Case 3: Alternating Polarity Phase Steps

Figure 18 illustrates the phase trajectory for Case 3a, where the phase toggles back and forth between 0 and pi radians along the portion of the constant-envelope circle in the upper half-plane in Figure 12. This case seems to be the most natural translation from BPSK to CPM: the CPM phase trajectory is simply a smoothed version of the classic BPSK trajectory where the '1' symbol is defined to have a phase of 0 radians and the '0' symbol has phase of π radians.

Figure 19 contains the spectrum for Case 3a. Notice the significant clock spurs that appear over the entire frequency range of the spectrum. The appearance of these spurs is understood by studying the signal diagram in Figure 12. Since the transitions are taking place entirely in the upper half plane, a positive pulse appears on the Q channel to mark the transition, whenever there is a transition, regardless of the symbol data. Since these pulses are independent of the PN data and occur at the symbol transition times, they result in the spectral spurs seen in the PSD in Figure 19. Therefore, Case 3a and 3b are not viable options due to the excessive spurs in the spectrum.

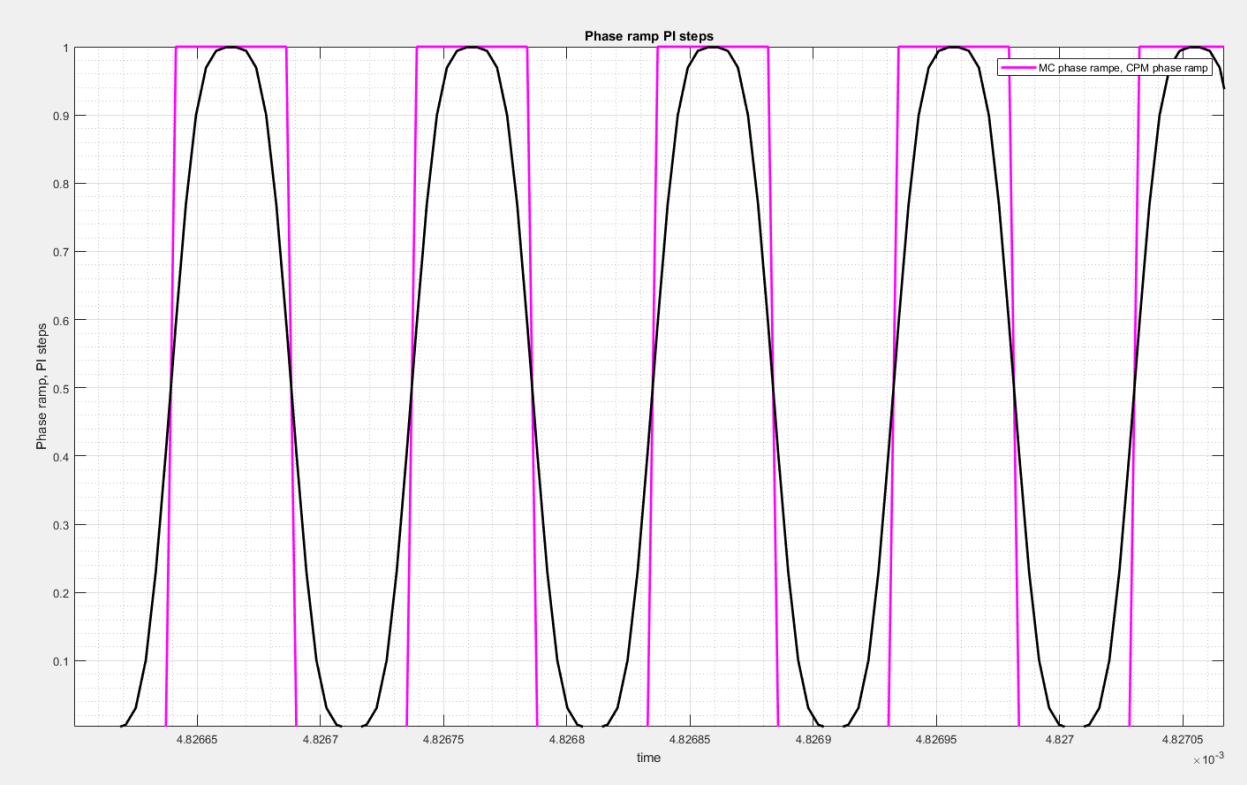

Figure 18: Phase trajectory for GCPM with alternating phase steps (simulation)

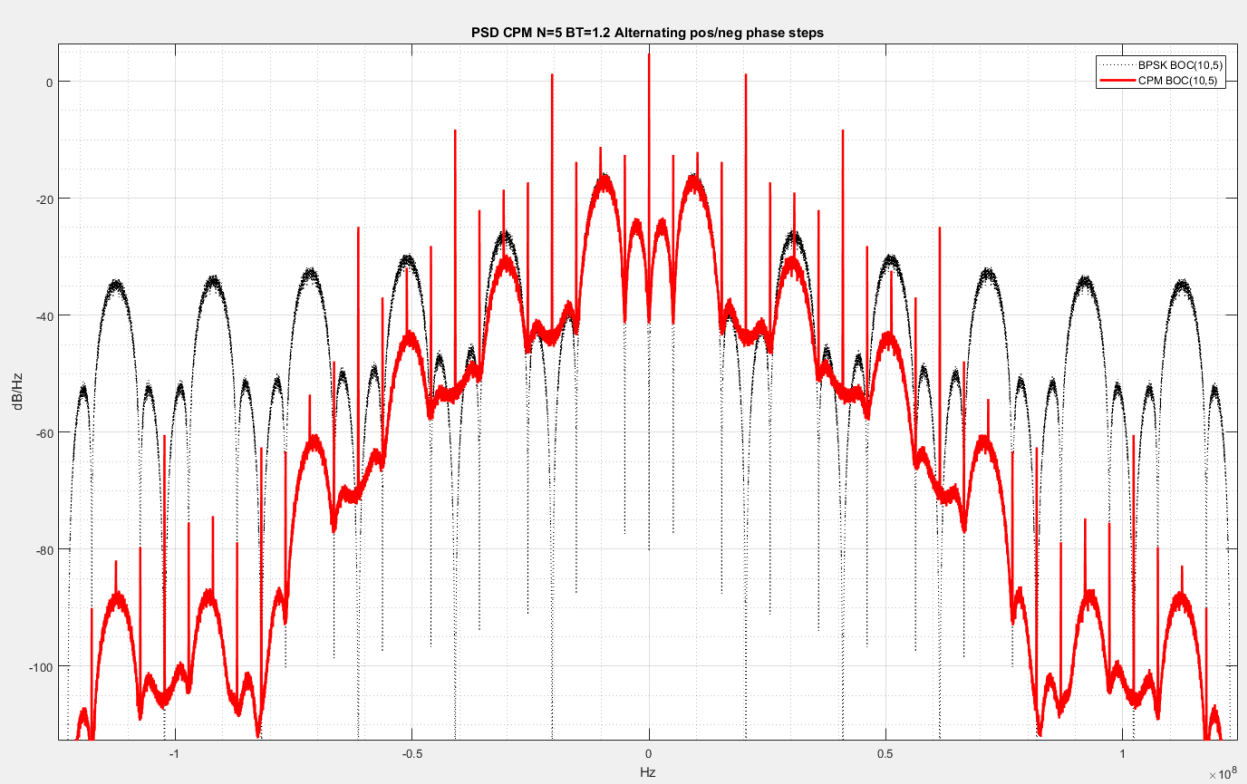

Figure 19: PSD for N=5, BT=1.2, GCPM with alternating polarity phase steps (simulation)

Case 4: Randomized Phase Transitions

Figure 20 shows the GCPM modulation process with one modification: the polarity of the phase shifts is randomized using a secondary PN generator. Randomizing the polarity of the phase steps results in the spectrum shown in Figure 21.

The cross correlation for this case is shown in Figure 22. Notice that the deep nulls in the correlation function at half-symbol offsets match those of BPSK BOC(10,5), indicating that the high precision ranging accuracy of the original BOC(10,5) waveform is preserved. The out-of-band power of the GCPM version is significantly reduced compared to BPSK. This is the solution we are looking for. The random phase transitions can be provided via a PN sequence, which is separate from the GPS code sequence. A US patent has been granted for this technique [7][8].

Note that the correlation peak of the N=5, BT=1.2, GCPM cross-correlation is 0.82dB lower than the BPSK version. This difference is the "correlation loss" of this version of GCPM. The modulation parameters N (width of pulse input to Gaussian filter) and BT (Gaussian filter bandwidth) can be adjusted to achieve a correlation loss that is compliant with the signal specification.

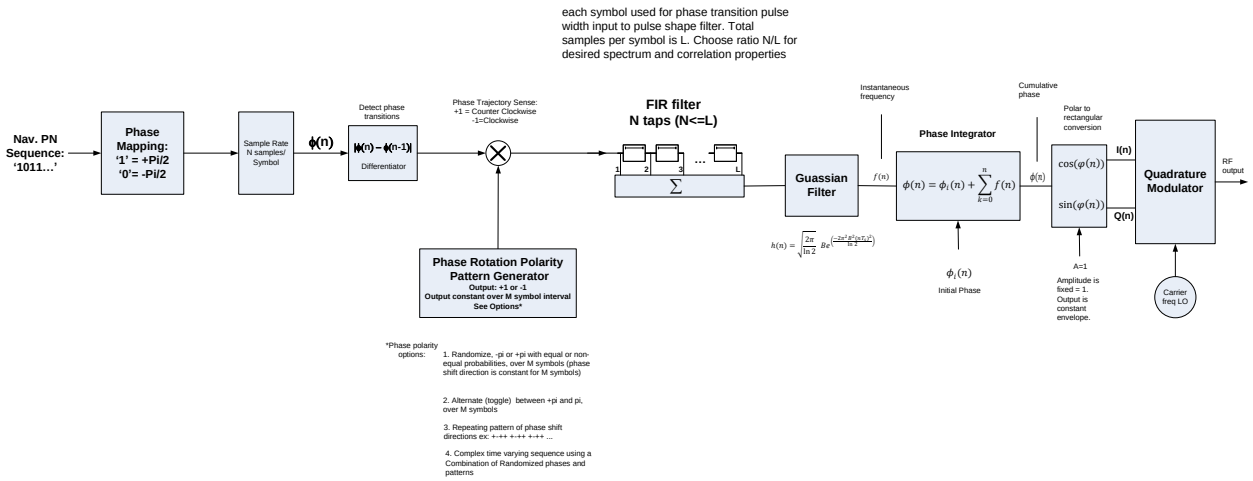

Figure 20: GCPM modulator with randomized phase transition polarity

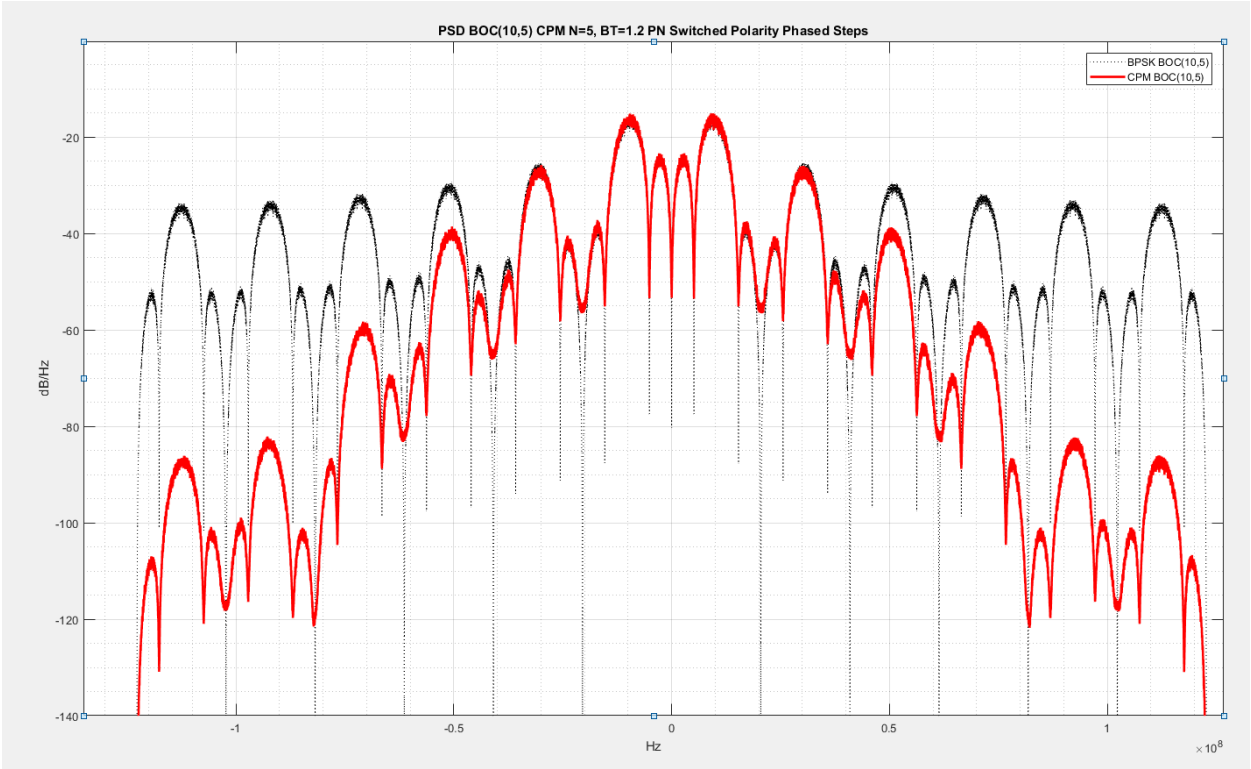

Figure 21: PSD for BOC(10,5) Gaussian GCPM with PN-randomized polarity phase steps (simulation)

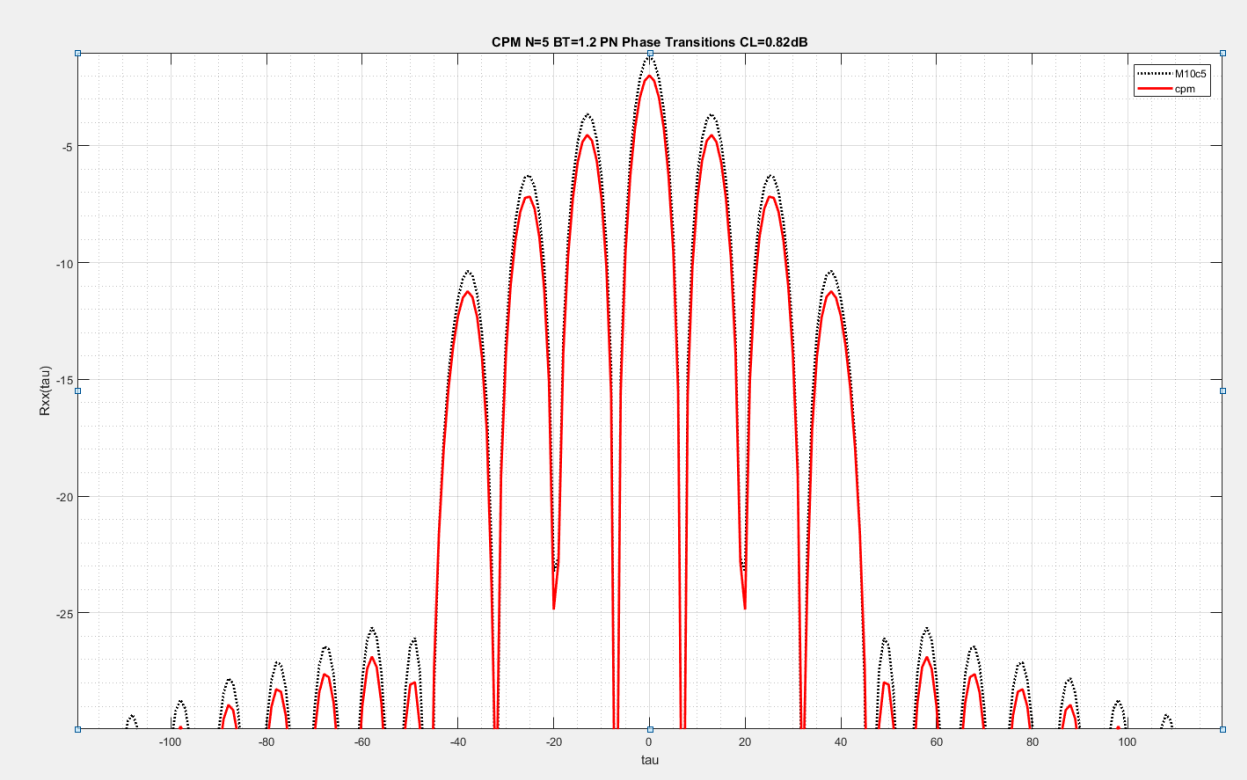

Figure 22: Cross-correlation between reference code and GCPM (N=5, BT=1.2) with PN-randomized polarity phase steps (simulation)

Performance of BOC(10,5) GCPM with Various Degrees of Phase Trajectory Shaping

Figures 23 and 24 show the phase trajectories and power spectra of three versions of the BOC(10,5) GCPM waveform compared with standard BPSK transmission. The GCPM modulation method shown in Figure 20 was employed, whereby frequency pulses are filtered by a Gaussian filter. As before, the phase transition smoothing is controlled by the frequency pulse width N and the filter bandwidth BT.

Figure 25 contains simulation data for truncation loss, max power spectral density in the 1600MHz radio astronomy (RA) band, and correlation loss for these same examples of GCPM based on simulation analysis. The RA band power illustrates how much the GCPM modulation is reducing the power in an adjacent service where GPS is required to keep emissions below a specified level. The reduction in PSD provided by GCPM is nearly 50dB for N=5. This translates to a relaxation of filtering requirements in this band, which in turn reduces the cost and risk of the design.

From Figures 23, 24, and 25 we can see that as N increases from 1 to 5, the phase trajectory becomes more gradual, the power spectrum rolls off more quickly with a commensurate decrease in truncation loss, and the correlation loss increases. The system designer can vary the N and BT parameters to generate a waveform that achieves the desired balance between bandwidth efficiency and correlation loss. The table in Figure 25 is an example of such a tradeoff for the GCPM BOC(10,5) signals analyzed here.

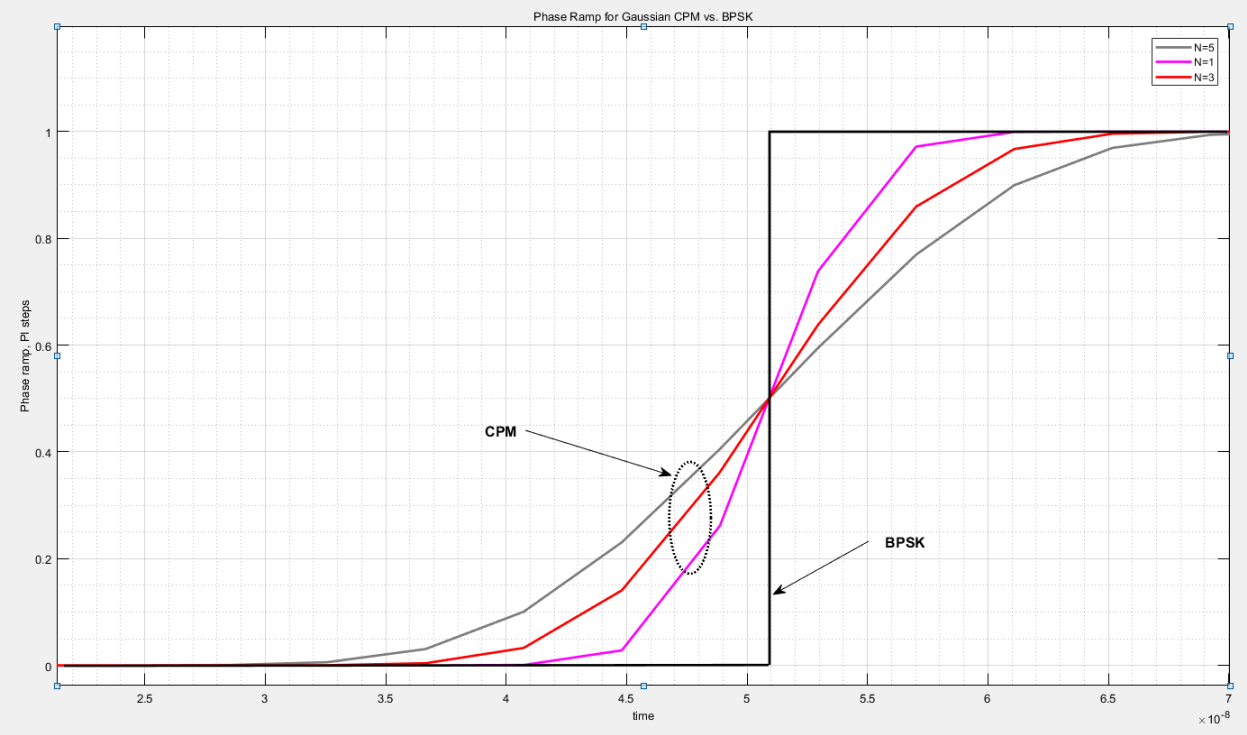

Figure 23: Phase trajectory of BOC(10,5) GCPM , N=1,3, and 5, BT=1.2 (simulation)

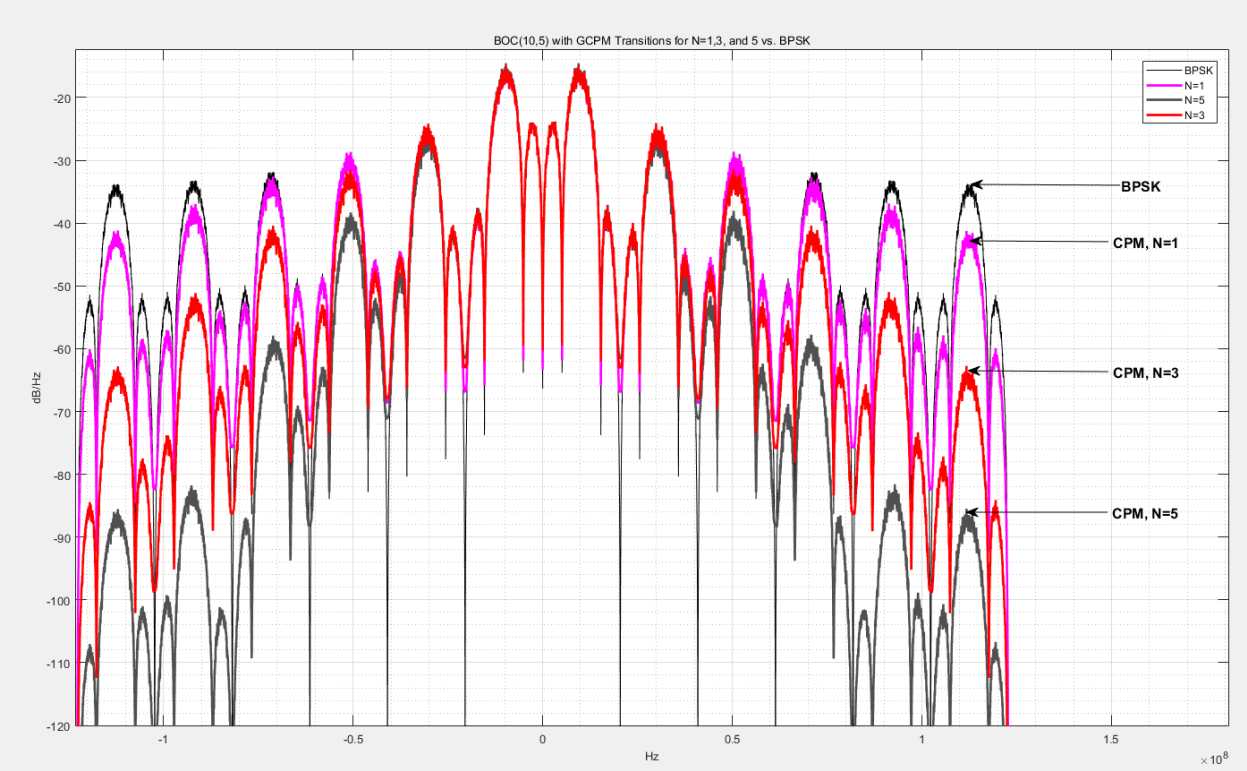

Figure 24: Spectrum of BOC(10,5) GCPM , N=1,3, and 5, BT=1.2 (simulation)

BOC(10,5) Modulation Type:	Truncation loss (power outside 30.69MHz bandwidth) dB	1660 - 1670MHz RA Band Max PSD dBm/Hz	Correlation Loss dB
BPSK	1.16	-33	0
GCPM N=1, BT=1.2	0.95	-47	0.39
GCPM N=3, BT=1.2	0.87	-56	0.54
GCPM N=5, BT=1.2	0.74	-82	0.82

Figure 25: Truncation loss, maximum PSD in 1660MHz RA band, and correlation loss, for BOC(10,5) GCPM , N=1,3, and 5, BT=1.2 (simulation)

The correlation loss shown in Figure 25 assumes a legacy receiver using a BPSK BOC(10,5) signal as the local reference for the correlation. If the receiver were updated to use a GCPM signal as its local reference, the correlation loss would be much lower.

Test Results

The BOC(10,5) CPM waveform defined here was tested using an L5 GPSIII transmitter EDU and an L1 GaN HPA. The resulting spectrum for the L5 EDU is shown in Figure 26. Note that the out-of-band spectral energy of the amplified CPM waveform has been reduced compared to the amplified standard BPSK BOC(10,5) waveform. The measured spectrum is similar to the simulation.

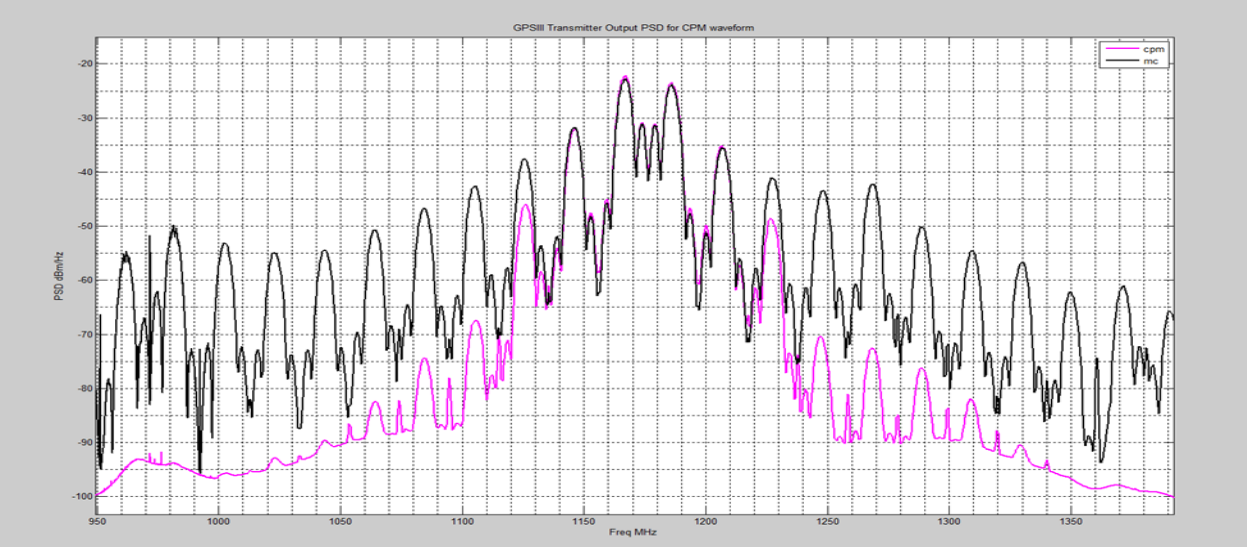

Figure 26: Output spectrum of L5 GPS transmitter for BPSK and CPM versions of the BOC(10,5) signal

Test results with the 250W L-band GaN HPA is shown in figures 27 and 28. We can see the PSD of the output of the GaN HPA for both BPSK BOC(10,5) and CPM, with N=5, BT=1.2. As predicted, the CPM modulation has reduced the out-of-band spectral content and the spectral regrowth is negligible.

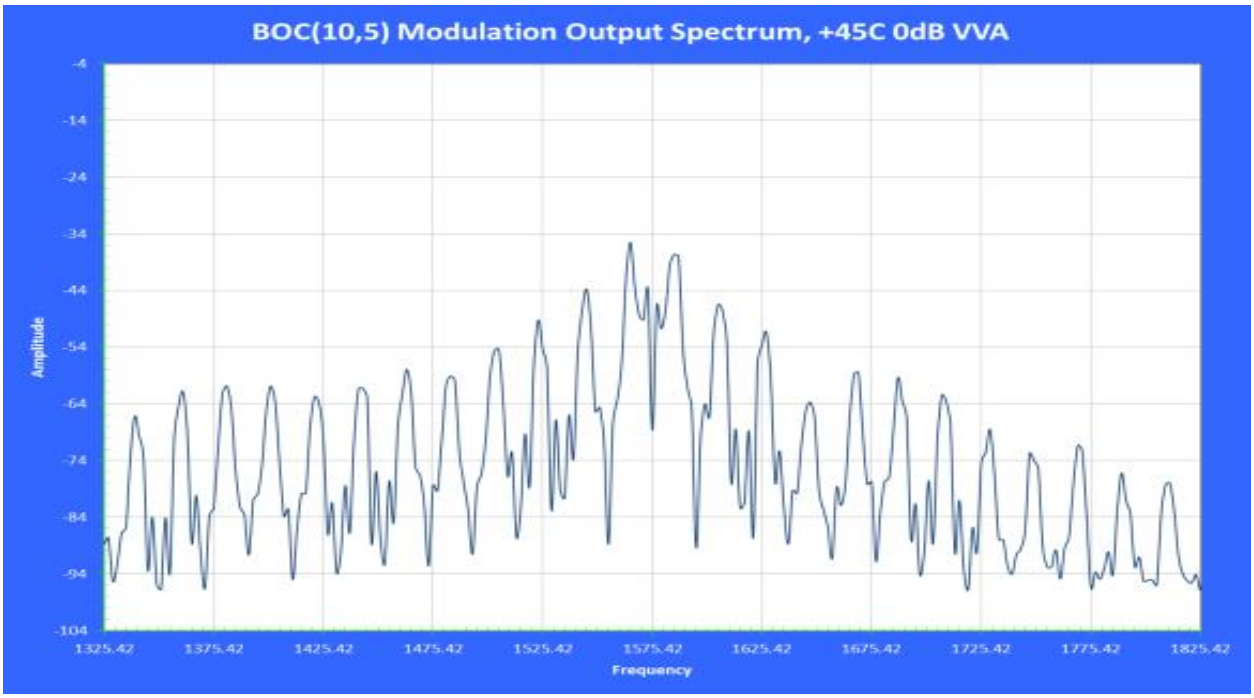

Figure 27: GaN HPA output spectrum for standard BPSK BOC(10,5) modulation

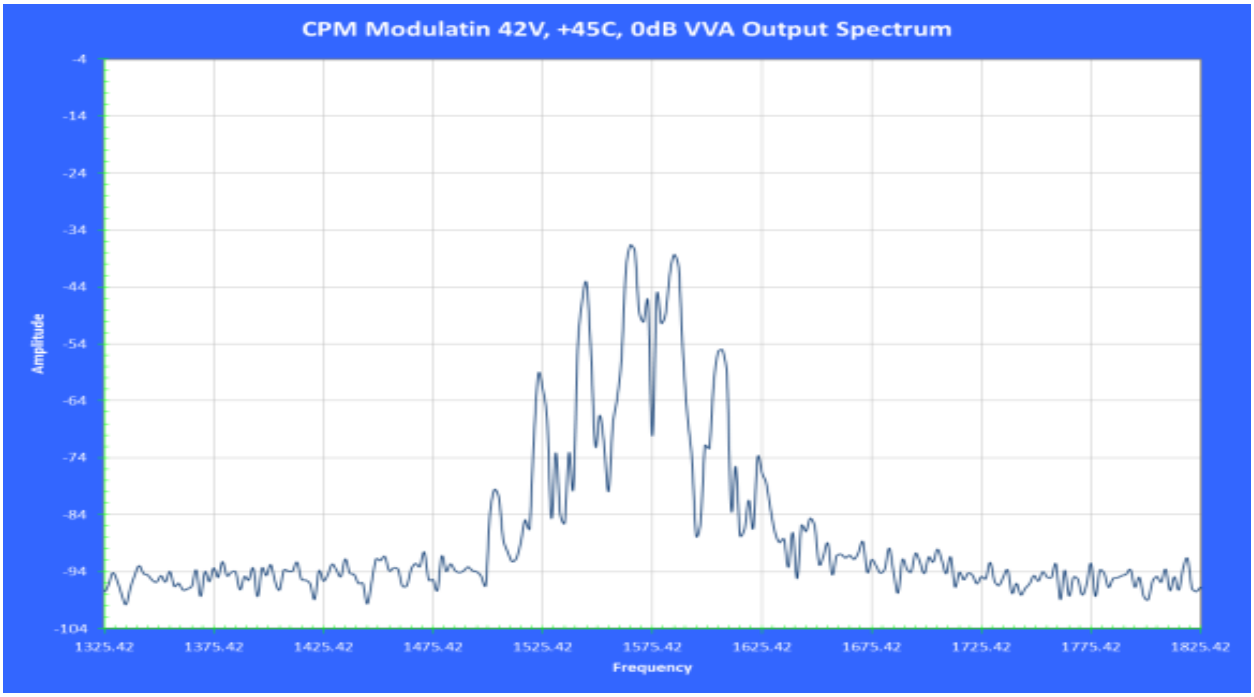

Figure 28: GaN HPA output spectrum for GCPM BOC(10,5) modulation

Figure 29 shows the efficiency and power output of the GaN HPA using CW, BPSK BOC(10,5) and CPM BOC(10,5) for N=5, BT=1.2. Notice the improved efficiency with CPM compared to BPSK. As the HPA approaches saturation, the CPM restores the efficiency to the CW level. Similarly, Figure 29 shows that the CPM BOC(10,5) restores the max power of the HPA to the CW level.

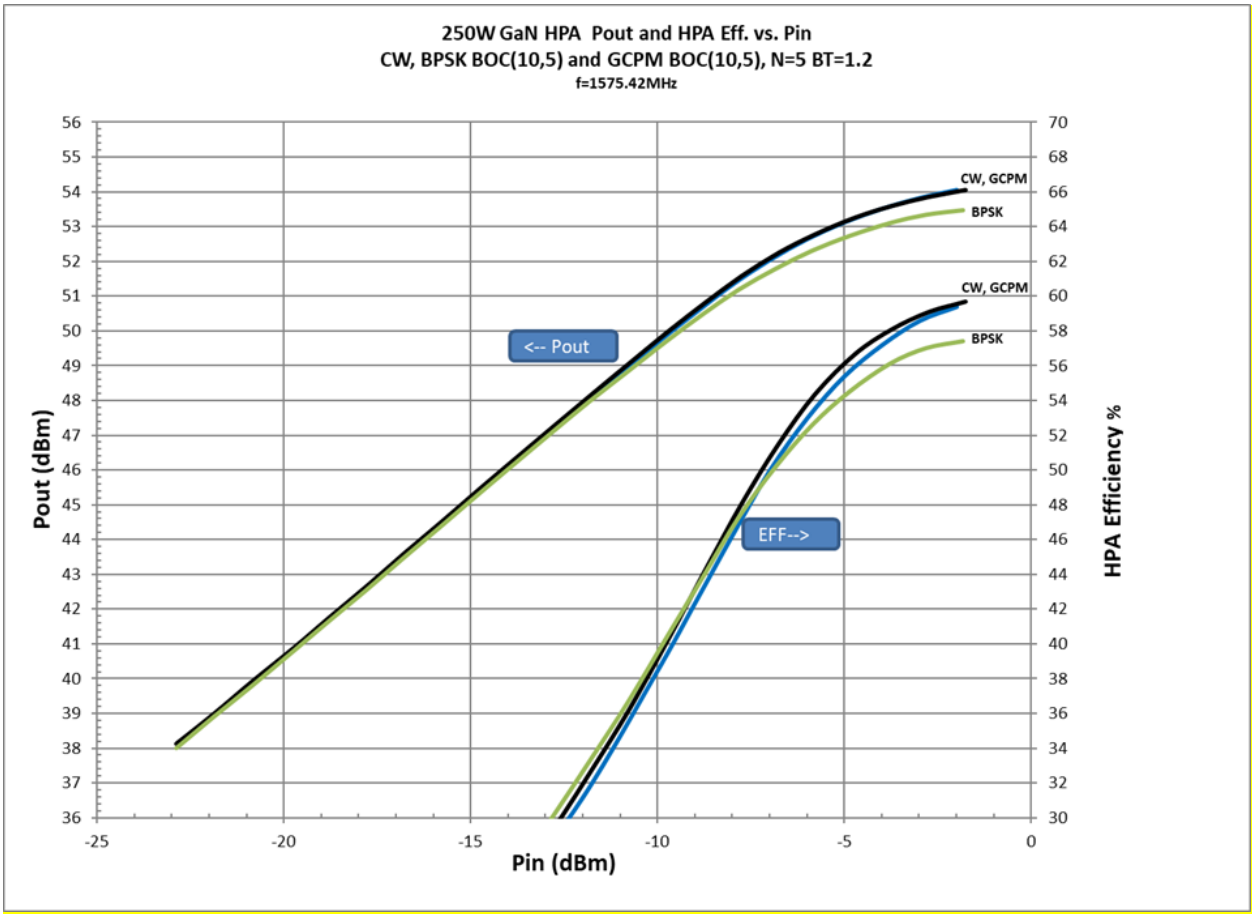

Figure 29: GaN HPA output power and efficiency for CW and BOC(10,5) with BPSK and GCPM (N=5, BT=1.2)

Application of Gaussian CPM to P(Y) and C/A Code

The same modulation technique may be used to generate bandwidth efficient versions of other GPS/GNSS codes. Figures 30 and 31 show spectra of the GCPM versions of the P(Y) and C/A codes. The P(Y) code uses N=4 out of 12 samples for the transition, with a Gaussian filter BT=1.5 The correlation loss is 0.33dB with a margin compared to the IS-GPS-200H requirement of 0.6dB.

The C/A code shown in Figure 31 uses a phase pulse transition, which is only 1/16 of the symbol, and a filter BT=6. Even with this modest degree of phase shaping, the results plotted in Figure 31 show a significant reduction in out-of-band power without filtering. The correlation loss for this waveform is 0.1dB, compared to the IS-GPS-200H requirement of 0.3dB.

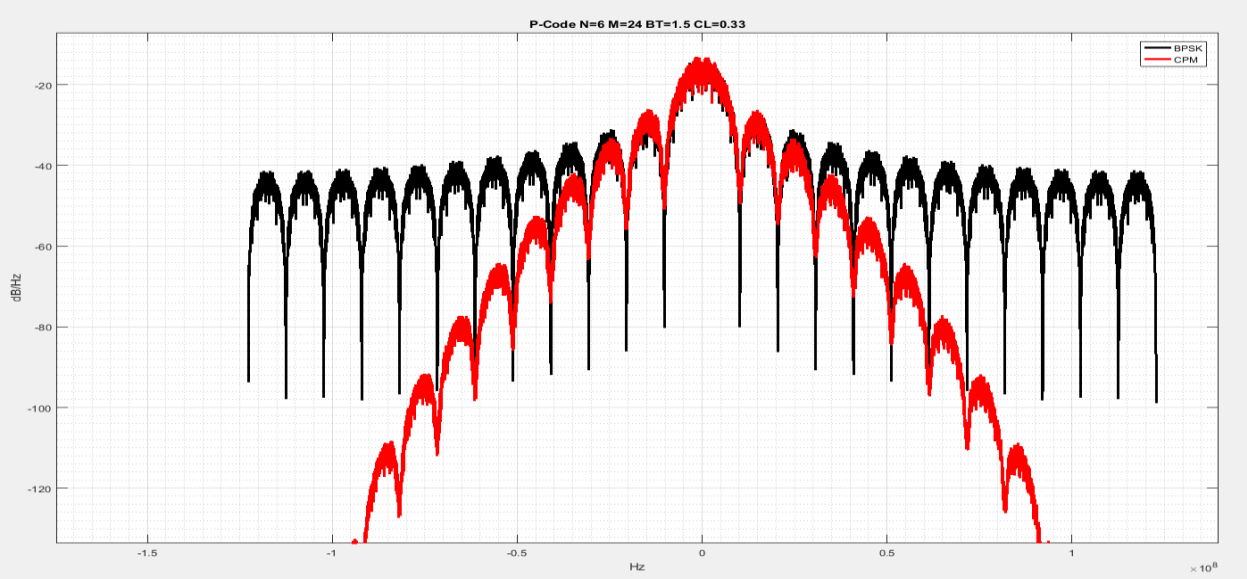

Figure 30: Spectrum of GCPM version of P(Y) code

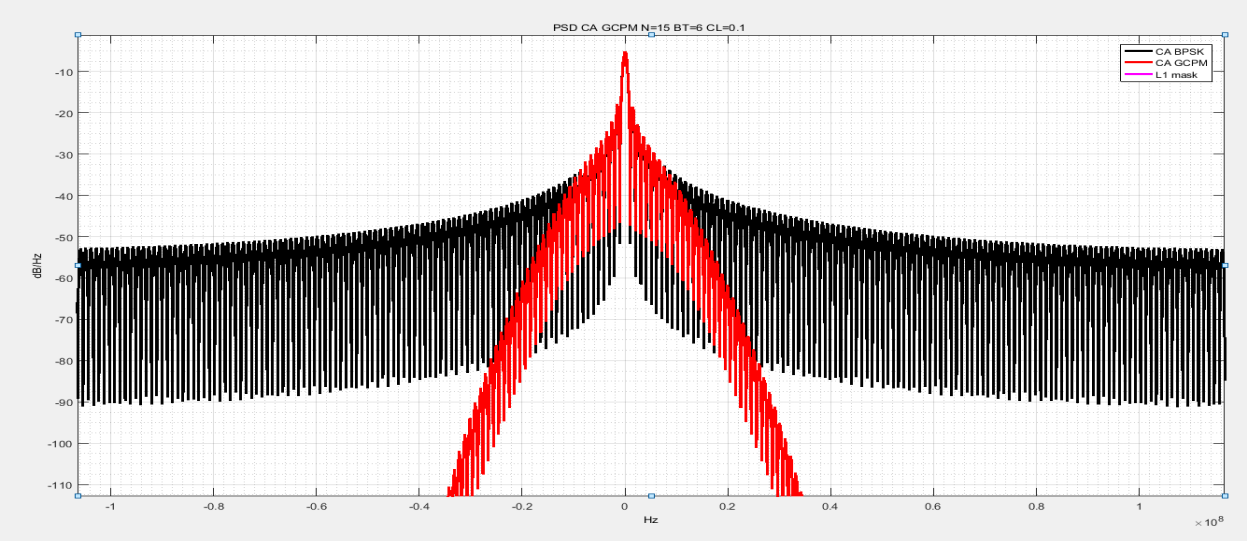

Figure 31: Spectrum of GCPM version of C/A code

Conclusion

This article has presented a CPM approach for generating GPS codes that are bandwidth efficient, yet can be used with a saturated RF amp for efficient RF/DC operation. The simulation and test results presented here use a Gaussian-pulse version of CPM (GCPM), but other pulse shapes, such as raised-cosine, could be used and the results should be similar. The GCPM waveforms have reduced out-of-band power and improved DC efficiency compared to BPSK. The BOC(10,5) code was used as the basis of comparison, but we also showed the performance improvement for GCPM versions of P(Y) and C/A codes. Using CPM for the GPS/GNSS codes could potentially enable the use of simplified post-HPA filters to achieve reduced complexity and filter losses.

The waveforms described in this work are only a subset of all the possibilities. Parameters such as the ratio N/L, BT, the pulse shape, and transition polarity patterns can each be adjusted to design a tailored waveform for each GNSS application.

The focus of this work was to produce backward-compatible GPS waveforms. Receivers could achieve even better correlation performance if modified to use the CPM versions of the waveform as the local reference code.

References

[1] GPS Interface Control Documents, https://www.gps.gov/technical/icwg/

[2] J. Betz, "The Offset Carrier Modulation for GPS Modernization". Proceedings of ION Technical meeting. Cambridge, Massachusetts: 639-648.

[3] J. Betz, "Binary Offset Carrier Modulations for Radionavigation," Journal of the Institute of Navigation, vol. 48

[4] E. Kaplan, C. Hegarty, "Understanding GPS Principles and Applications"

[5] B. Barker, John Betz, et al., "Overview of the GPS M-Code Signal"

[6] J. Proakis, "Digital Communications", Fourth Edition

[7] P. S. Kossin, "Bandwidth Efficient Continuous Phase Modulation", U.S. Patent 9 571 317, February 14, 2017

[8] P. S. Kossin, "Continuous Phase Modulation for GPS Codes", ION Joint Navigation Conference, 2017